Demixing in simple dipolar mixtures: Integral equation versus density functional results

Gabriel M. Range* and Sabine H. L. Klapp†

Stranski-Laboratorium für Physikalische und Theoretische Chemie, Sekretariat TC 7, Fakultät II für Mathematik und Naturwissenschaften, Technische Universität Berlin, Straße des 17. Juni 124, D-10623 Berlin, Germany

(Received 13 February 2004; published 21 September 2004)

Using reference hypernetted chain (RHNC) integral equations and density functional theory in the modified mean-field (MMF) approximation we investigate the phase behavior of binary mixtures of dipolar hard spheres. The two species (*A* and *B*) differ only in their dipole moments m_A and m_B, and the central question investigated is under which conditions these asymmetric mixtures can exhibit *demixing* phase transitions in the fluid phase regime. Results from our two theoretical approaches turn out to strongly differ. Within the RHNC (which we apply to the isotropic high-temperature phase) demixing does indeed occur for dense systems with small interaction parameters $\Gamma = m_B^2/m_A^2$. This result generalizes previously reported observations on demixing in mixtures of dipolar and neutral hard spheres ($\Gamma = 0$) to the case of true dipolar hard sphere mixtures. The RHNC approach also indicates that these demixed fluid phases are isotropic at temperatures accessible by the theory, whereas isotropic-to-ferroelectric transitions occur only at larger Γ. The MMF theory, on the other hand, yields a different picture in which demixing occurs *in combination* with spontaneous ferroelectricity at all Γ considered. This discrepancy underlines the relevance of correlational effects for the existence of demixing transitions in dipolar systems without dispersive interactions. Indeed, supplementing the dipolar interactions by small, asymmetric amounts of van der Waals–like interactions (and thereby supporting the systems tendency to demix) one finally reaches good agreement between MMF and RHNC results.

DOI: 10.1103/PhysRevE.70.031201 PACS number(s): 77.80.−e, 64.70.−p, 61.25.Em, 64.75.+g

I. INTRODUCTION

Phase transitions in fluids are very sensitive to the nature of intermolecular interactions, and this is particularly true for fluids involving permanent molecular dipole moments. In fact, recent theoretical research has shown that even most simple dipolar model fluids can display new and unexpected phase behavior, such as spontaneous polarization in dense liquid states [1–4] and self-assembly of the particles into chains with head-to-tail aligned dipoles in the dilute gas [5–8]. Chain formation is particularly pronounced in dipolar fluids without additional dispersive interactions, such as dipolar hard spheres (DHS's) [6–8], where *conventional* gas-liquid coexistence (which has been expected since the angle-averaged dipolar interaction between two particles is attractive) is indeed absent [9]. Against this background it seems somewhat counterintuitive that mixtures of DHS's and neutral hard spheres (HS's) have been shown [10–12] to exhibit conventional *demixing* phase transitions, indicating that the effect of dipolar forces in mixtures may be very different from that in pure fluids.

In the present study we are concerned with the appearance of demixing phase transitions in binary mixtures of DHS with the two species *A* and *B* differing only in the magnitude of the dipole moments m_A and m_B (i.e., the size of particles is the same in each component). Though not particulary realistic as a model for polar molecular mixtures, binary DHS fluids do have relevance for ferrocolloids which are commonly characterized by a nonuniform distribution of dipole moments [13]. Moreover, the present model, of which the DHS-HS mixture considered previously [10–12] is just a limiting case ($m_B = 0$), allows us to investigate directly the influence of the anisotropic dipolar interactions on demixing phenomena, contrary to most other studies of dipolar mixtures involving usually models with additional dispersive interactions (see, e.g., [14] and [15]). Indeed, given that pure DHS fluids (or mixtures with $m_B = m_A$) polarize spontaneously at sufficiently large densities and coupling strengths, a question of particular importance is not only whether true mixtures with $m_B \neq m_A$ demix at all, but also whether they demix already in the *isotropic* phase.

To address these topics we employ in this study two different theoretical approaches, that is reference hypernetted chain (RHNC) integral equation theory and density functional theory in the modified mean-field (MMF) approximation.

The RHNC theory is used to calculate approximate two-particle correlation functions in the homogeneous isotropic fluid phase. Combining this structural information with an appropriate stability analysis we then *predict* the low-temperature phase behavior on the basis of diverging fluctuations. Their direction in the space of order parameters indicates the character of the transition (e.g., isotropic-to-ferroelectric and/or demixing transitions). Previous applications of this approach have shown that the phase behavior of DHS fluids observed in computer simulations is correctly predicted [16–18], including the existence of isotropic demixing transitions in DHS-HS mixtures [11,12]. One may therefore expect reasonable results for true binary DHS fluids as well. We note that, at least for the isotropic phases, it is in principle possible to analyze the phase behavior directly on the basis of RHNC phase coexistence curves

*Electronic address: gabriel.range@fluids.tu-berlin.de
†Electronic address: sabine.klapp@fluids.tu-berlin.de

 ©2004 The American Physical Society

following from the RHNC chemical potentials and pressure [19]. These calculations, however, would imply a substantial additional effort. In the present study we are interested mainly in the qualitative phase behavior rather than in the actual location of phase coexistence curves.

Within the MMF approach, on the other hand, phase diagrams are determined more directly by minimizing a free energy functional, where two-particle correlations are approximated by the Boltzmann factor [20–22]. In a previous paper [23] we have presented a detailed investigation of the global MMF phase behavior (within the fluid range) of DHS mixtures. Here we focus on comparison of the results to those from the RHNC stability analysis. Indeed, while the main advantage of the MMF is that both isotropic and polarized phases can be easily included, interparticle correlations are handled on a much simpler level than in the integral equation theory. Comparison of the two approaches therefore provides useful insight concerning the importance of correlational effects for the phase behavior. Indeed, our results suggest that *isotropic* DHS mixtures can demix (under appropriate thermodynamic conditions), but that these demixing transitions are rather subtle phenomena in that they disappear within the MMF approach.

The rest of the paper is organized as follows. In Sec. II we formulate the model and present main expressions of the two theoretical approaches employed, including an explicit expression (plus derivation in the Appendix) for the dielectric constant of the dipolar mixture. Numerical results obtained within the RHNC and MMF theories are presented in Secs. III A and III B, respectively. It turns out that the predictions differ qualitatively when strongly asymmetric DHS mixtures are considered. Therefore, we finally discuss systems with additional spherically symmetric interactions, for which the RHNC and MMF approaches become roughly consistent again. Our conclusions are summarized in Sec. IV.

II. THEORY

A. Model

We consider binary mixtures of two species (A and B) of dipolar hard spheres with equal diameters σ but different dipole moments m_A and m_B. In addition to the dipole-dipole interaction a Lennard-Jones (LJ) interaction between the spheres may be present as well. The resulting pair potential between two particles with coordinates $(1)=(\mathbf{r}_1,\omega_1)$ and $(2)=(\mathbf{r}_2,\omega_2)$ is given as

$$u_{ab}(12)=\begin{cases}\infty, & r_{12}<\sigma,\\ u_{ab}^{\mathrm{dip}}(\mathbf{r}_{12},\omega_1,\omega_2)+u_{ab}^{\mathrm{LJ}}(r_{12}), & r_{12}>\sigma,\end{cases} \tag{2.1}$$

where $r_{12}=|\mathbf{r}_{12}|=|\mathbf{r}_2-\mathbf{r}_1|$ is the particle separation, $\omega=(\theta,\phi)$ represents the orientation of a dipole in a spatially fixed coordinate system, and the subscripts a and b denote the components considered $[a,b=A,B]$. The dipolar potential is given by

$$u_{ab}^{\mathrm{dip}}(\mathbf{r}_{12},\omega_1,\omega_2)=\frac{m_a m_b}{r_{12}^3}\{\hat{\mathbf{m}}(\omega_1)\cdot\hat{\mathbf{m}}(\omega_2)-3[\hat{\mathbf{m}}(\omega_1)\cdot\hat{\mathbf{r}}_{12}]\times[\hat{\mathbf{m}}(\omega_2)\cdot\hat{\mathbf{r}}_{12}]\}, \tag{2.2}$$

where $\hat{\mathbf{m}}(\omega)$ and $\hat{\mathbf{r}}_{12}$ are unit vectors in the direction of ω and $\mathbf{r}_{12}$, respectively. Finally,

$$u_{ab}^{\mathrm{LJ}}(r_{12})=4\epsilon_{ab}\left[\left(\frac{\sigma}{r_{12}}\right)^{12}-\left(\frac{\sigma}{r_{12}}\right)^{6}\right] \tag{2.3}$$

is the LJ potential. Setting $\epsilon_{ab}=0$ the pair potential (2.1) reduces to that of DHS mixtures. For finite attraction parameters ϵ_{ab} the present model is a slightly modified version of a Stockmayer fluid mixture (see, e.g., Ref. [14]); the additional hard core has been introduced for numerical convenience.

B. RHNC stability analysis

A main concern of the present work is the mixtures phase behavior at large (but still fluidlike) total densities $\rho=\rho_A+\rho_B$ (with $\rho_a=N_a/\mathcal{V}$). Based on previous studies of two limiting cases—that is, mixtures with only one dipolar component ($m_B=0$) [10–12], on the one hand, and one-component dipolar fluids ($\rho_B\to 0$) [1–4], on the other hand—one would expect these systems, upon cooling from a mixed isotropic high-temperature phase, to either *demix* or *spontaneously polarize* or exhibit a combination of these phase transitions. Condensation transitions seem also possible, especially when systems with isotropic interactions are considered (i.e., $\epsilon_{ab}>0$) [14]. In order to properly characterize the phase behavior based on information of the isotropic high-temperature state (which can be treated by standard integral equation techniques [24]), we apply a stability analysis developed by Chen and Forstmann [11,12]. Contrary to other frameworks such as Kirkwood-Buff theory [25], the general analysis of Chen and Forstmann gives us a rigorous criterion on which we can decide whether it is demixing or condensation or an orientational instability which dominates the phase behavior.

The central idea is to consider the change $\delta\Omega=\Omega-\Omega^{\mathrm{eq}}$ of the grand canonical free energy induced by density fluctuations $\delta\rho_a(1)$ around the homogeneous and isotropic equilibrium state, characterized by constant singlet densities $\rho_a(1)=\rho_a/4\pi$. Up to second order, $\delta\Omega$ is given by

$$\delta\Omega\approx\frac{1}{2}\sum_{ab}\int d1\int d2\,\delta\rho_a(1)\left.\frac{\delta^2\Omega}{\delta\rho_a(1)\delta\rho_b(2)}\right|_{\mathrm{eq}}\delta\rho_b(2)=\frac{k_BT}{2}\sum_{ab}\int d1\int d2\,\delta\rho_a(1)\left[\frac{\delta_{ab}\delta(12)}{\rho_a/4\pi}-c_{ab}(12)\right]\delta\rho_b(2), \tag{2.4}$$

where k_B is Boltzmann's constant, T is the temperature, δ_{ab} is the Kronecker delta, and $c_{ab}(12)$ is the direct correlation function at equilibrium. For each (small) fluctuation, the corresponding value of $\delta\Omega$ determines the "restoring force." Stability (or metastability) therefore implies that $\delta\Omega$ is *positive* for fluctuations with arbitrary directions in density space.

Expression (2.4) can be simplified by introducing Fourier transforms of the density fluctuations and correlation func-

tions, respectively, and expanding these quantities along angle-dependent basis functions [12]. Choosing the wave vector $\mathbf{k}$ along the polar axis ("$\mathbf{k}$ frame"), the density expansion reads $\delta\tilde{\rho}_a(\mathbf{k},\omega_1)=\Sigma_{l_1,\chi}\,\delta\rho_a^{l_1,\chi}(k)Y_{l_1,\chi}(\omega_1)$, where $k=|\mathbf{k}|$ and the $Y_{l_1,\chi}(\omega_1)$ are spherical harmonics. Furthermore, one has $\tilde{c}_{ab}(\mathbf{k},\omega_1,\omega_2)=\Sigma_{l_1l_2}\,\Sigma_\chi\,\tilde{c}_{ab}^{l_1l_2,\chi}(k)\Psi^{l_1l_2,\chi}(\omega_1,\omega_2)$, where $-\min(l_1,l_2)\leqslant\chi\leqslant\min(l_1,l_2)$ and the $\Psi^{l_1l_2,\chi}$ are rotational invariants defined in Appendix 3B of Ref. [24]. Equation (2.4) then transforms to

$$\delta\Omega=\frac{2\pi k_BT}{V}\sum_{\mathbf{k}}\sum_{\chi}\sum_{ij}\delta\overline{\rho}_{i,\chi}^{*}(k)[\mathbf{M}_\chi(k)]_{ij}\delta\overline{\rho}_{j,\chi}(k), \quad (2.5)$$

where we have introduced the combinations of indices $i=(a,l_1)$ and $j=(b,l_2)$, and the fluctuations $\delta\overline{\rho}_{i,\chi}(k)=\delta\rho_a^{l_1,\chi}(k)/\sqrt{\rho_a}$. Furthermore, the elements of the matrices $\mathbf{M}_\chi(k)$ are defined as

$$[\mathbf{M}_\chi(k)]_{ij}=\delta_{ij}-(-1)^\chi\sqrt{\frac{\rho_a\rho_b}{(2l_1+1)(2l_2+1)}}\,\tilde{c}_{ab}^{l_1l_2,\chi}(k). \quad (2.6)$$

Due to symmetries of the coefficients $\tilde{c}_{ab}^{l_1l_2,\chi}(k)$, the matrices $\mathbf{M}_\chi(k)$ are real and symmetric and $\mathbf{M}_\chi(k)=\mathbf{M}_{-\chi}(k)$.

The structure of Eq. (2.5) implies that fluctuations with different wave numbers k and angular indices χ are decoupled. Stability therefore requires *all* matrices $\mathbf{M}_\chi(k)$ to be positive definite, which can be easily checked by an investigation of the eigenvalues. In the stable (or metastable) system all eigenvalues are positive. Phase transitions are indicated by an eigenvalue going to zero (upon decreasing T, for example), reflecting that there is a direction in density space along which the restoring force for fluctuations becomes particularly small. Identifying that eigenvalue and monitoring the related direction in density space we can thus predict the character of the phase transition under consideration.

Practically, the direct correlation functions determining $\mathbf{M}_\chi(k)$ are calculated via numerical solution of the Ornstein-Zernike equations [12,26] for the isotropic fluid mixture combined with the reference hypernetted chain closure approximation (involving Verlet-Weis [27] hard sphere correlation functions). The details of these calculations can be found elsewhere (see, e.g., Refs. [28,16]). Here we note that our numerical solution scheme implies a truncation of the expansion of $\tilde{c}(1,2)$ at $l_1^{\max}=l_2^{\max}=2$ and therefore $|\chi|^{\max}=2$. The matrices $\mathbf{M}_0(k)$, $\mathbf{M}_{\pm1}(k)$, and $\mathbf{M}_{\pm2}(k)$ then have dimensions 6×6, 4×4, and 2×2, respectively.

1. Most important instabilities

Since we are mainly interested in demixing or condensation and in isotropic-to-ferroelectric transitions, long-wavelength ($k\to0$) fluctuations of the number densities (angular indices $l_i=\chi=0$) and the polarizations ($l_i=1$, $\chi=0,\pm1$) are particularly important. We can discuss these fluctuations separately from each other (and from other fluctuations), since the matrices $\mathbf{M}_0(0)$ and $\mathbf{M}_{\pm1}(0)$ have block form with respect to the indices l_i.

For number density fluctuations we therefore consider the 2×2 submatrix $\mathbf{D}_0$ of $\mathbf{M}_0(0)$ with elements

$$[\mathbf{D}_0]_{ab}=\delta_{ab}-\sqrt{\rho_a\rho_b}\,\tilde{c}_{ab}^{00,0}(0). \quad (2.7)$$

A vanishing of the smaller eigenvalue λ_D of $\mathbf{D}_0$ indicates demixing *or* condensation of the system. This can be clarified by investigating the direction of the eigenvector related to λ_D in the two-dimensional space spanned by $[\boldsymbol{\delta\rho}]_1=\delta\rho_A^{0,0}(0)/\sqrt{\rho_A}$ and $[\boldsymbol{\delta\rho}]_2=\delta\rho_B^{0,0}(0)/\sqrt{\rho_B}$. Pure *condensation* occurs if the eigenvector lies along direction $\mathbf{x}_\rho=(\sqrt{\rho_A},\sqrt{\rho_B})$, since the projection

$$\boldsymbol{\delta\rho}\cdot\mathbf{x}_\rho=\delta\rho_A^{0,0}(0)+\delta\rho_B^{0,0}(0)=\delta\rho \quad (2.8)$$

corresponds to a fluctuation of the *total* number density. On the other hand, pure demixing (with fixed total density) is indicated by an eigenvector along direction $\mathbf{x}_c=\rho^{-2}(\sqrt{\rho_A}\,\rho_B-\sqrt{\rho_B}\,\rho_A)\perp\mathbf{x}_\rho$, since

$$\boldsymbol{\delta\rho}\cdot\mathbf{x}_c=\sqrt{\rho_B}\,\delta\rho_A^{0,0}(0)-\sqrt{\rho_A}\,\delta\rho_B^{0,0}(0)=\delta c \quad (2.9)$$

is a pure concentration fluctuation. By monitoring the angle α between the eigenvector and, say, $\mathbf{x}_c$ we can thus predict the type of transition the system approaches.

We now turn to polarization fluctuations related to the 2×2 submatrices $\mathbf{F}_0$ and $\mathbf{F}_1$ of $\mathbf{M}_0(0)$ and $\mathbf{M}_{\pm1}(0)$ with elements

$$[\mathbf{F}_0]_{ab}=\delta_{ab}-\frac{\sqrt{\rho_a\rho_b}}{3}\tilde{c}_{ab}^{11,0}(0),$$

$$[\mathbf{F}_1]_{ab}=\delta_{ab}+\frac{\sqrt{\rho_a\rho_b}}{3}\tilde{c}_{ab}^{11,1}(0). \quad (2.10)$$

Ferroelectric transitions of the mixture are indicated when the smaller eigenvalue λ_F of $\mathbf{F}_1$ goes to zero. To see this we consider the physical precursor of ferroelectric order—that is, the mixture's dielectric constant ϵ. This quantity is related to matrices (2.10) by

$$\epsilon=\frac{\det\mathbf{F}_0}{\det\mathbf{F}_1}, \quad (2.11)$$

where "det" denotes the determinant. A derivation of Eq. (2.11) can be found in the Appendix. Numerical investigation shows that $\det\mathbf{F}_0$ remains finite at all states considered. Therefore, a vanishing of the smaller eigenvalue λ_F of $\mathbf{F}_1$ can be uniquely related to a divergence of the dielectric constant,

$$\epsilon\to\infty \quad\Leftrightarrow\quad \lambda_F\to0, \quad (2.12)$$

which indicates an isotropic-to-ferroelectric transition. The direction of the eigenvector related to λ_F indicates which component "drives" the transition; usually this will be the component with stronger dipolar interactions.

C. Modified mean-field density functional theory

As a supplement of the RHNC stability analysis, which is based on the homogeneous isotropic phase and thus yields only indirect information on the overall phase behavior, we also perform modified mean-field density-functional calculations. The great advantage of this approach, which we have decribed in detail in Ref. [23], is that ferroelectric phases (as

TABLE I. The coefficients $u_{ab,l}^{(n)}$ [see Eq. (2.18)] for $l,n\leqslant 4$. The quantities $I_{ab}^{(n)}$ follow from numerical integration of Eq. (2.19).

	$n=0$	$n=1$	$n=2$	$n=3$	$n=4$
$l=0$	$-(8\pi/\beta)I_{ab}^{(0)}$	0	$-(8\pi\beta/3)I_{ab}^{(0)}$	0	$-(8\pi\beta^3/25)I_{ab}^{(4)}$
$l=1$	0	$-(8\pi/27)$	0	$-(16\pi\beta^2/225)I_{ab}^{(3)}$	0
$l=2$	0	0	$-(8\pi\beta/375)I_{ab}^{(2)}$	0	$-(32\pi\beta^3/6125)I_{ab}^{(4)}$
$l=3$	0	0	0	$(16\pi\beta^2/25725)I_{ab}^{(3)}$	0
$l=4$	0	0	0	0	$-(8\pi\beta^3/99225)I_{ab}^{(4)}$

long as they are spatially homogeneous) can be easily included. We thus consider fluid states with singlet densities

$$\rho_a(\mathbf{r}_1,\omega_1)=\frac{\rho_a}{2\pi}\overline{\alpha}_a(\cos\,\theta)=\frac{\rho_a}{2\pi}\left(\frac{1}{2}+\sum_{l=1}^{\infty}\alpha_{a,l}\,\mathcal{P}_l(\cos\,\theta)\right), \tag{2.13}$$

where $\overline{\alpha}_a(\cos\,\theta)$ is a normalized orientational distribution function $[\int_{-1}^{1}dx\overline{\alpha}_a(x)=1]$, and θ is the angle relative to the director of the orientational order (if present). Consequently, we can expand the distribution in Legendre polynomials $\mathcal{P}_l$ [see second line in Eq. (2.13)], where the coefficients $\alpha_{a,l}$ are connected to the usual lth-rank order parameters $P_{a,l}$ via

$$P_{a,l}=\int_{-1}^{1}dx\overline{\alpha}_a(x)\mathcal{P}_l(x)=\frac{2}{2l+1}\alpha_{a,l}. \tag{2.14}$$

The isotropic phase is specified by $P_{a,l\geqslant 1}=0$—i.e., $\overline{\alpha}_a(x)=1/2$—whereas a ferroelectric phase is characterized by $P_{a,l}\neq 0$ for all l.

Employing Eq. (2.13), the grand canonical density functional Ω of the mixture is given by [23]

$$\frac{\Omega}{\mathcal{V}}=\sum_a\frac{\rho_a}{\beta}[\ln(\rho_a\Lambda_a^3)-1]+\sum_a\frac{\rho_a}{\beta}\int_{-1}^{1}dx\overline{\alpha}_a(x)\ln[2\overline{\alpha}_a(x)]$$
$$+\frac{\rho}{\beta}\frac{4\eta-3\eta^2}{(1-\eta)^2}+\frac{F^{\mathrm{ex}}}{\mathcal{V}}-\sum_a\mu_a\rho_a, \tag{2.15}$$

where the first two terms on the right-hand side of Eq. (2.15) correspond to the ideal (translational and orientational) part of the free energy, and the third term is the Carnahan-Starling expression [29] for the hard sphere reference system (with packing fraction $\eta=\pi\rho\sigma^3/6$). Furthermore, F^{ex} is the excess free energy (see below), and the last term in Eq. (2.15) contains the chemical potentials μ_a controlling the composition of the mixture.

The MMF approximation [20,30] consists in setting the pair distribution function $g_{ab}(12)$ involved in the *exact* expression for F^{ex} equal to its low density limit—i.e., $g_{ab}(12)\rightarrow\exp[-\beta u_{ab}(12)]$. The implementation of this approximation into the density functional is described in detail in Ref. [23], and essentially the same derivations can also be used for the present system (which differs from that considered previously [23] only by the presence of additional LJ interactions). As a result, the excess free energy reduces to a quadratic form in the densities and order parameters,

$$\frac{F^{\mathrm{ex}}}{\mathcal{V}}=\sum_{ab}\rho_a\rho_b\sum_{l=0}^{\infty}u_{ab,l}\;\alpha_{a,l}\;\alpha_{b,l}, \tag{2.16}$$

where $\alpha_{a,0}=1/2$ and the coupling parameters are given as a power series in terms of the dipole moments—that is,

$$u_{ab,l}=\sum_{n=0}^{\infty}u_{ab,l}^{(n)}(m_am_b)^n. \tag{2.17}$$

For $n\neq 1$, the temperature-dependent coefficients $u_{ab,l}^{(n)}$ appearing in Eq. (2.17) are defined by

$$u_{ab,l}^{(n)}=-\frac{1}{2\beta}\frac{1}{4\pi^2n!}(-\beta)^nI_{ab}^{(n)}\int d\omega_1\,d\omega_2\,d\omega_{12}\,\mathcal{P}_l(\cos\,\theta_1)$$
$$\times\mathcal{P}_l(\cos\,\theta_2)\tilde{\Phi}_{112}^{n}(\omega_1,\omega_2,\omega_{12}), \tag{2.18}$$

where the $I_{ab}^{(n)}$ are (short-range) spatial integrals,

$$I_{ab}^{(n)}=\int_{\sigma}^{\infty}dr_{12}\frac{1}{r_{12}^{3n-2}}\{\exp[-\beta u_{ab}^{\mathrm{LJ}}(r_{12})]-\delta_{n0}\}, \tag{2.19}$$

which can be easily evaluated by standard numerical integration techniques. Furthermore, the angular integrals in Eq. (2.18) can be solved by expressing both the Legendre polynomials and the quantities $\tilde{\Phi}_{112}^{n}$ [where $\tilde{\Phi}_{112}=\hat{\mathbf{m}}_1\cdot\hat{\mathbf{m}}_2-3(\hat{\mathbf{m}}_1\cdot\hat{\mathbf{r}}_{12})(\hat{\mathbf{m}}_2\cdot\hat{\mathbf{r}}_{12})$] by spherical harmonics as described in Ref. [23].

Finally, the coefficient corresponding to $n=1$ in Eq. (2.17) is related to an integral over the long-range dipolar potential itself and therefore requires special treatment. One finally obtains (see Ref. [23] and references therein)

$$u_{ab,l}^{(1)}=-\frac{8\pi}{27}\delta_{l,1}. \tag{2.20}$$

In practice, we truncate the Taylor expansion appearing in Eq. (2.17) at $n_{\max}=4$. Explicit expressions for the resulting set $(l,n\leqslant 4)$ of coefficients $u_{ab,l}^{(n)}$ [after performing the angular integrals in Eq. (2.18)] are given in Table I. Inserting Eqs. (2.17) and (2.16) into Eq. (2.15) completes our construction of the MMF density functional. In order to identify the set of ten parameters $(\{\rho_a,\alpha_{a,1},\ldots,\alpha_{a,4}\})$ characterizing the equilibrium state at given $(\mu_a,T,\mathcal{V})$, we solve the Euler-Lagrange equations

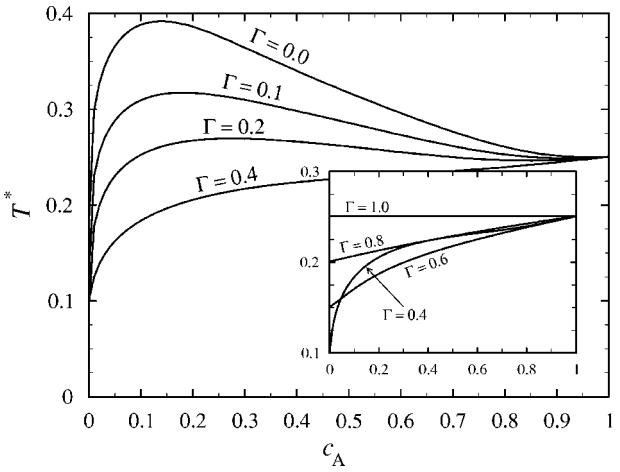

FIG. 1. Stability limits of binary DHS mixtures with interaction ratios $\Gamma \leqslant 0.4$ and $\Gamma \geqslant 0.4$ (inset) in the concentration-temperature plane ($T^* = k_B T \sigma^3 / m_A^2, c_A = \rho_A / \rho$). The total density is fixed at $\rho^* = 0.7$.

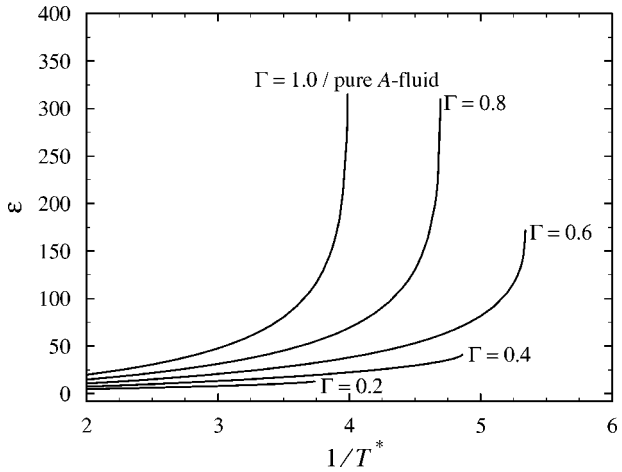

FIG. 2. Dielectric constant as function of the inverse temperature for the pure A fluid and for mixtures at $c_A = 0.2$ and various values of Γ.

$$\frac{\partial (\Omega/\mathcal{V})}{\partial \rho_a} = 0, \quad \frac{\delta(\Omega/\mathcal{V})}{\delta \overline{\alpha_a}(x)} = 0. \tag{2.21}$$

This is done numerically by employing a multidimensional Newton-Raphson algorithm. Moreover, *coexisting states* at given chemical potentials μ_A and μ_B are identified by combining Eqs. (2.21) with a further equation reflecting that the pressures $p = -\Omega^{\mathrm{eq}}(\mu_A, \mu_B, T)/\mathcal{V} = -\Omega[\rho_a^{\mathrm{eq}}, \overline{\alpha}_a^{\mathrm{eq}}(x)]/\mathcal{V}$ of both states have to be equal as well.

III. RESULTS AND DISCUSSION

A. RHNC stability analysis of DHS mixtures

Most of our RHNC results have been obtained for DHS mixtures without additional LJ interactions [i.e., $\epsilon_{ab} = 0$ in Eq. (2.3)]. These systems can be characterized by the reduced temperature $T^* = k_B T \sigma^3 / m_A^2$, the interaction parameter $\Gamma = m_B^2 / m_A^2$ specifying the different dipolar couplings within the two species, the reduced total density $\rho^* = (\rho_A + \rho_B)\sigma^3$, and the concentration of the A component, $c_A = \rho_A / \rho$. All calculations have been carried out at fixed total density $\rho^* = 0.7$. This value has already been considered in previous RHNC integral equation [11,12] and Monte Carlo simulation [10] studies for the limiting case $\Gamma = 0$, which corresponds to a mixture where the B particles are just hard spheres. In the present study we consider systems at seven different interaction parameters in the range $0 \leqslant \Gamma \leqslant 1$, where $\Gamma = 1$ is again a special case in that the corresponding mixtures are essentially one-component DHS fluids for all concentrations $0 \leqslant c_A \leqslant 1$. We also note that the behavior of mixtures with $\Gamma > 1$ follows from the present systems by interchanging A and B.

For each Γ we have first determined the stability limits (spinodals) of the mixed isotropic fluid phase—i.e., the temperatures $T_s^*(c_A)$ where one of the eigenvalues discussed in Sec. II B 1 approaches zero upon lowering T^* towards T_s^*. Results are shown in Fig. 1. All of the lines approach the same limiting value for $c_A \to 1$, corresponding to the temperature where pure isotropic DHS fluids become unstable due to an isotropic-to-ferroelectric transition. This is illustrated in Fig. 2 where the behavior of the dielectric constant upon $T^* \to T_s^*$ is displayed for various values of Γ, including $\Gamma = 1$ where the actual value of c_A is irrelevant. The appearant divergence of ϵ at $\Gamma = 1$ indicates formation of a low-temperature fluid phase with *spontaneous* long-range parallel ordering of the dipole moments, and this prediction is consistent with various computer simulation results [1–4]. A comparison of the actual transition temperatures indicates that RHNC theory overestimates the tendency for ferroelectric ordering, but still yields the best theoretical results so far [16].

Turning back to Fig. 1 we note that the ferroelectric instability of the pure system reappears (except for $\Gamma = 0$) on the left-hand side of the diagrams ($c_A \to 0$), since these systems are again one-component DHS fluids at $\rho^* = 0.7$ but with dipole moments $m_B \leqslant m_A$ and therefore $T_s^*(c_A = 0) = \Gamma\, T_s^*(c_A = 1) \leqslant T_s^*(c_A = 1)$. In the two subsequent paragraphs we discuss in detail the behavior of true *mixtures* of DHS's with compositions in between the limiting cases $c_A \to 0, 1$.

1. Mixtures with $\Gamma \geqslant 0.4$

Typical for mixtures with relatively large interaction parameters $0.4 \leqslant \Gamma < 1$ is that replacing A particles more and more by B particles—i.e., decreasing c_A from the limiting value 1 (pure A fluid), yields a *monotonic* decrease of T_s^* as illustrated in the inset of Fig. 1. Furthermore, when considering a fixed concentration—say, $c_A = 0.2$ (see Fig. 2)—the dielectric constant ϵ continues to diverge as it does in the pure A system, suggesting that the ferroelectric transition is preserved. Further evidence for this behavior is seen in Fig. 3 where we have plotted the eigenvalues λ_{F} [see Eq. (2.12)] and λ_{D} [see Eq. (2.7) below] as functions of the inverse temperature for two differently composed mixtures at a representative interaction ratio ($\Gamma = 0.8$). For both mixtures, the fluctuations related to λ_{D} are found to be mainly *concentration* fluctuations; i.e., numerical values of the angle α be-

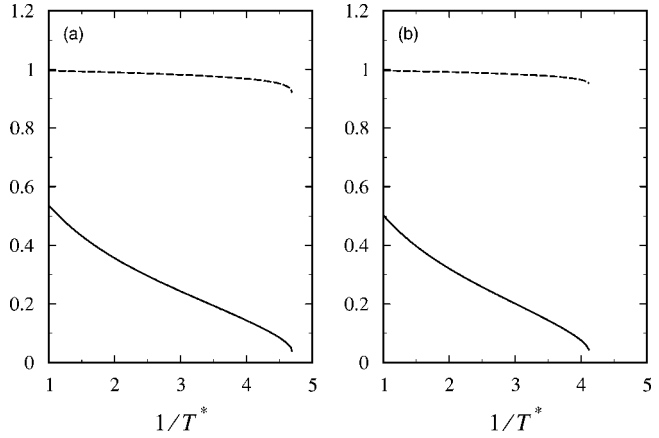

FIG. 3. The eigenvalues λ_F (solid lines) and λ_D (dashed lines) as functions of the inverse temperature at $\Gamma=0.8$ and $c_A=0.2$ (a) and $c_A=0.8$ (b).

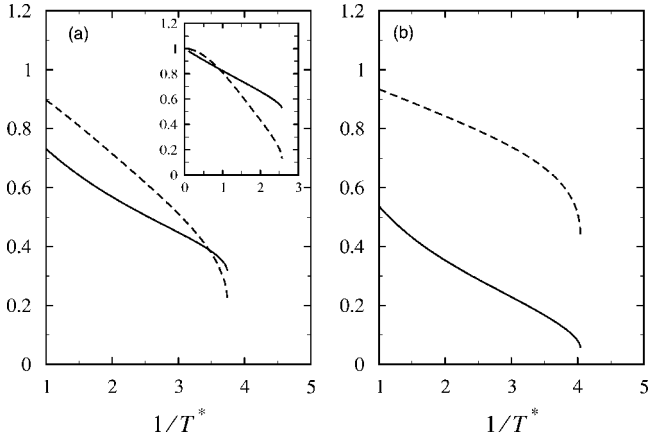

FIG. 4. The eigenvalues λ_F (solid lines) and λ_D (dashed lines) as functions of the inverse temperature at $\Gamma=0.2$ and $c_A=0.2$ (a) and $c_A=0.8$ (b). The inset of (a) shows results for $c_A=0.2$ and $\Gamma=0$.

tween the fluctuation vector $\boldsymbol{\delta\rho}$ and the direction of pure concentration fluctuations $\mathbf{x}_c$ [see Eq. (2.8) below] are very small. Comparing, however, the actual magnitude and temperature dependence of λ_D in Fig. 3 to that of λ_F one concludes that the concentration fluctuations have minor importance against those of the polarization, which diverge when approaching T_s^* (as indicated by the sudden decrease of λ_F). Thus, the origin of the stabilitiy limits in Fig. 1 (inset) is indeed spontaneous polarization rather than a demixing within the isotropic phase, even though the decrease of λ_D suggests that the isotropic-to-ferroelectric transitions may be accompanied by small changes in the composition of the system. In fact, given that the *A* particles are more strongly coupled one would actually expect the low-temperature ferroelectric phase to be characterized by somewhat higher values of c_A (and, also, ρ). Finally, having identified the ferroelectric character of the stability limits in Fig. 1 (inset) it is plausible that the stability limit of the isotropic phase indeed decreases (for a fixed Γ) when *A* particles are replaced by (less strongly coupled) *B* particles.

2. Mixtures with $\Gamma \leqslant 0.4$

Mixtures with more asymmetric dipolar couplings exhibit a different physical behavior as indicated already by the *shape* of the spinodals displayed in the main part of Fig. 1: upon decreasing c_A from 1 the temperatures T_s^* first *rise* and start to decrease only at some (Γ-dependent) small value of the concentration of *A* particles. Also, as seen from Fig. 2, the dielectric constant at small concentrations c_A remains small for all temperatures considered, suggesting that the stability limit of these systems is not (at least not primarily) related to a ferroelectric transition. In order to get a clearer picture we investigate again the eigenvalues λ_F and λ_D, taking now the case $\Gamma=0.2$ as an example. In Fig. 4 the eigenvalues are plotted for two different concentrations, the smaller of which is in the range where the stability limit goes through the maximum. The corresponding results [see Fig. 4(a)] clearly show that it is now λ_D which goes to zero significantly faster than λ_F (contrary to what we have seen before). Furthermore, the related angle α (see Table II for some representative values) is close to zero, indicating that the diverging fluctuations related to λ_D are essentially concentration (rather than total density) fluctuations. The small *negative* values of α merely suggest that the phase richer in *A* particles will also be somewhat denser (which seems sensible due to the stronger coupling within the *A* species). Figure 4(b) finally shows that the situation changes again at larger c_A in that polarization fluctuations become dominating for $T^* \to T_s^*$. These *A*-rich systems thus transform directly into ferroelectric phases as do the mixtures with large Γ discussed in Sec. III A 1.

Taken altogether, our results indicate that strongly asymmetric DHS mixtures characterized by *intermediate* values of c_A may exhibit demixing phase transitions *without* simultaneous ferroelectric ordering (even though one would actually expect the demixed fluid phases to undergo a second phase transition of ferroelectric type at some lower temperatures). It seems then obvious that the demixing tendency becomes even more pronounced upon further decrease of the interaction ratio. That this is indeed the case is demonstrated in Figs. 5(a)–5(d) where we have plotted, for four different values of Γ, the values of λ_D and λ_F obtained *directly* at the stability limit. Compared to $\Gamma=0.2$ [cf. Fig. 5(c)], the range of c_A where λ_D is the smallest eigenvalue (thus indicating demixing) significantly broadens when Γ is decreased [see Figs. 5(a) and 5(b)], the largest window occurring for $\Gamma=0$ corresponding to a mixture of DHS's and pure hard spheres. Representative results for the temperature behavior of the eigenvalues at $\Gamma=0$ are displayed in the inset of Fig. 4. The data clearly reveal the dominance of concentration fluctuations over those of the polarization. We note that the case

TABLE II. Numerical values of the angle α [see Eq. (2.9) below] at the stability limit corresponding to $c_A=0.2$ and different values of Γ. Pure concentration (total density) fluctuations correspond to $\alpha=0°(90°)$.

$\Gamma=0.0$	$\Gamma=0.1$	$\Gamma=0.2$	$\Gamma=0.4$
$-2.11°$	$-2.91°$	$-3.62°$	$-4.85°$

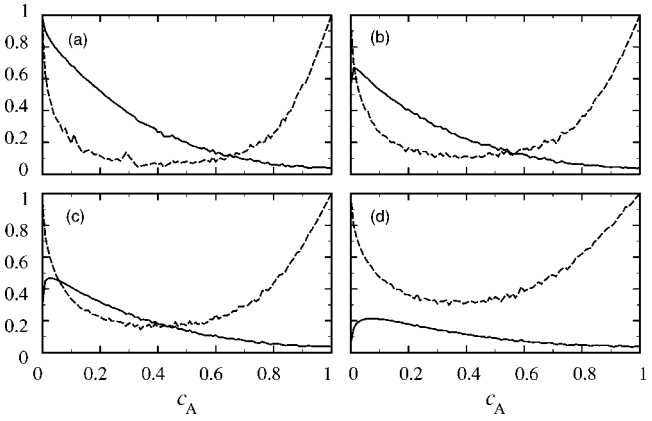

FIG. 5. Eigenvalues λ_F (solid lines) and λ_D (dashed lines) at the stability limits for $\Gamma=0$ (a), $\Gamma=0.1$ (b), $\Gamma=0.2$ (c), and $\Gamma=0.4$ (d).

$\Gamma=0$ has also been investigated previously both by RHNC integral equations [11,12] (with which studies our own results are consistent) and by Monte Carlo computer simulations [10]. The latter have confirmed the occurrence of demixing transitions, including that the resulting phases are indeed *isotropic* as suggested by the theory. It seems thus safe to assume that the RHNC stability analysis is also correct in predicting isotropic demixing transitions for true dipolar mixtures with small, but finite values of Γ.

B. MMF density functional results

Given the severe approximation for the interparticle correlations within the MMF theory it is interesting to see to which extent this approach reproduces the RHNC predictions for the phase behavior, particularly in context with demixing transitions. We focus on the case $\Gamma=0$ (DHS-HS mixture) where the tendency to demix into two isotropic phases is largest. Also, apart from "hard core" systems without isotropic attractions (i.e., $\epsilon_{ab}=0$ as in Sec. III A) we consider in addition one example where the *A* component is a Stockmayer fluid as defined in Eq. (2.1).

From a technical point of view comparison between the RHNC and MMF results is complicated by the fact that, instead of ρ^* and c_A, the reduced chemical potentials $\mu_a^* = \beta\mu_a - \ln(\Lambda_a^3/\sigma^3)$ of the two species are the natural input for the MMF calculations along with the temperature T^*. We handle that point such that we first consider density-temperature MMF phase diagrams of the fluid phase regime obtained at fixed chemical potential difference $\Delta\mu^* \equiv \mu_B^* - \mu_A^*$. Based on these diagrams we then extract concentration-temperature diagrams at *fixed* total density in order to make contact with the RHNC results (see Fig. 1).

1. Mixtures without isotropic attraction

Density-temperature phase diagrams for $\Gamma=0$ and $\epsilon_{ab}=0$ are plotted in Fig. 6 where the different curves belong to different values of the parameter $\Delta\mu^*$. In the limit $\Delta\mu^* \to -\infty$ one recovers the MMF phase diagram of the pure *A* fluid containing only two fluid phases—that is, an isotropic gas (IG) and a ferroelectric liquid (FL). Below the temperature

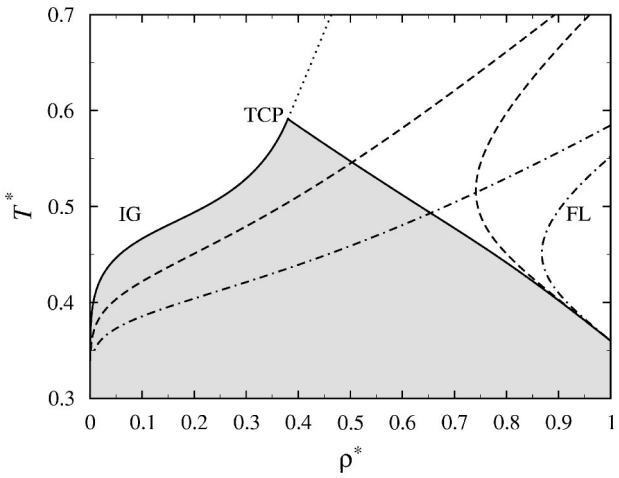

FIG. 6. MMF density-temperature phase diagrams for DHS-HS mixtures ($\Gamma=0$) at $\Delta\mu^* \to -\infty$ (solid and dotted lines), $\Delta\mu^*=2.0$ (dashed lines), and $\Delta\mu^*=4.0$ (dot-dashed lines). The abbreviations are explained in the main text.

T^*_{TCP} related to the *tricritical point* (TCP), the transition between the two phases is of first order both in density and in the orientational order parameters $\alpha_{A,l>1}$. Above T^*_{TCP} the IG-FL transition becomes continuous. The resulting *critical line* separating the isotropic and ferroelectric phase can be found from a Landau analysis as described in Refs. [20,23].

Starting from the pure *A* behavior, one apparent change induced by increasing $\Delta\mu^*$ is a shift of the isotropic-to-ferroelectric transition. Indeed, when considering mixtures at fixed total density (or fixed temperature) one finds from Fig. 6 that the IG-FL transition moves towards lower temperatures (or higher densities) with increasing $\Delta\mu^*$. Since increase of $\Delta\mu^*$ implies *decrease* of the concentration of *A* particles the results in Fig. 6 also imply that, at fixed density, the ferroelectric transition temperatures decrease with decreasing c_A. This is seen more directly in Fig. 7 where the transition temperatures at $\rho^*=0.7$ are plotted as functions of

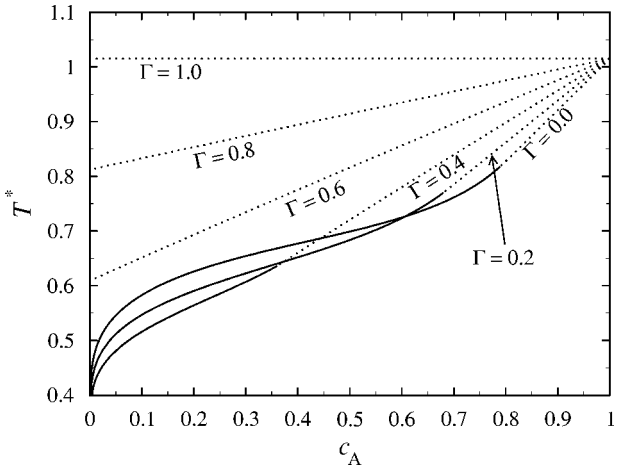

FIG. 7. MMF results for the temperatures related to the boundary of the isotropic phase at $\rho^*=0.7$ and various values of Γ. Dashed (solid) lines denote second-order (first-order) phase transitions.

the concentration c_A corresponding to different $\Delta\mu^*$. The results indicate destabilization of ferroelectric ordering when the dipolar *A* particles are replaced by hard sphere *B* particles.

A second change upon increasing $\Delta\mu^*$ concerns the *order* of the IG-FL transition which, as seen from both Figs. 6 and 7, becomes discontinuous for all temperatures and densities corresponding to the fluid phase regime. This concerns not only density and polarization but also the concentration c_A (not shown), the values of which in the coexisting IG and FL phases are observed to become very different, particularly for large $\Delta\mu^*$ (where the FL phase is dominated by *A* particles). We stress, however, that regardless of the value of $\Delta\mu^*$ or ρ^* considered, jumps in c_A are always accompanied by spontaneous polarization. In other words, the MMF approach does not reproduce demixing phase transitions *within* the isotropic phase observed both in the RHNC stability analyis (see Sec. III A and Refs. [11,12]) and in computer simulations [10].

Given this discrepancy at $\Gamma=0$ where the mixtures tendency to demix is largest anyway, it is not surprising to find similar differences between the MMF and RHNC predictions at finite interaction ratios (MMF results at finite Γ have been obtained by us previously in Ref. [23]). Some MMF results for the boundaries of the isotropic high-temperature phase at $\Gamma>0$ are included in the c_A-T^* diagram in Fig. 7 (density $\rho^*=0.7$). For all cases considered the corresponding (first- or second-order) phase transformations are isotropic-to-ferroelectric transitions, with the transition temperature decreasing monotonically on decreasing c_A. This is in contrast to the RHNC spinodals (see Fig. 1) which, for sufficiently small Γ, exhibit a maximum related to demixing transitions without an accompanying isotropic-to-ferroelectric transition. One should also note, however, that MMF and RHNC theories do give consistent results at larger Γ. This concerns both the shape of the phase boundaries and their origin—that is, spontaneous polarization—even though there are obvious differences in the actual predictions for the ferroelectric transition temperatures. For example, at $\Gamma=0.8$, $c_A=0.2$ the ferroelectric transition temperature predicted by the RHNC is approximately 4 times smaller than the corresponding MMF result. On the other hand, both approaches predict the orientationally ordered phase to be characterized by larger values of c_A and ρ^*.

2. Influence of additional dispersive interactions

In view of the shortcomings of the MMF theory in predicting isotropic demixing transitions in strongly asymmetric DHS mixtures we conclude this study by a brief discussion of a system where dipolar interactions are supplemented by *weak* LJ interactions. Specifically, we consider a mixture of Stockmayer spheres (*A*) and hard spheres (*B*) characterized by $\epsilon_{BB}=\epsilon_{AB}=0$ and $\epsilon_{AA}\sigma^3/m_A^2=:\epsilon_{AA}^*=0.3$. This value of ϵ_{AA}^*, which reflects that the isotropic attraction between *A* particles is much smaller than their mutual dipolar interaction, is quite realistic for a number of polar molecular fluids [31]. The resulting MMF density-temperature $(T^*=k_BT\sigma^3/m_A^2)$ phase diagram of the *pure A* fluid (or the mixture in the limit $\Delta\mu^*\to-\infty$) is plotted in Fig. 8(a) from which one concludes

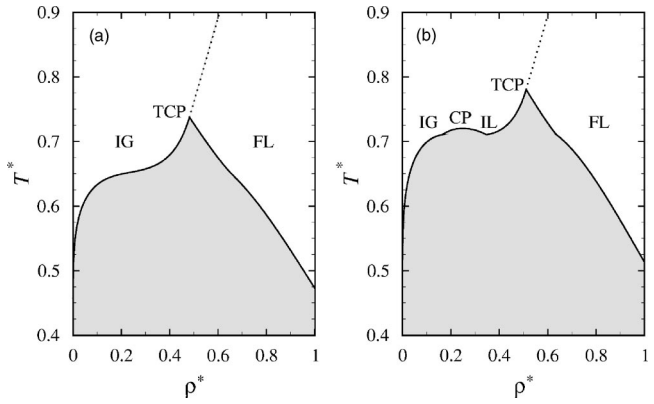

FIG. 8. MMF density-temperature phase diagrams of pure (*A*) Stockmayer fluids characterized by $\epsilon_{AA}^*=0.3$ (a) and $\epsilon_{AA}^*=0.4$ (b).

that the system, similarly to the pure DHS fluid (cf. Fig. 6) does *not* display phase coexistence between an IG and an isotropic liquid (IL). This changes, of course, upon increasing the attraction, and an example can be seen in Fig. 8(b) where we present the phase diagram of the pure *A* fluid at $\epsilon_{AA}^*=0.4$ (CP denotes the IG-IL critical point). However, since we are interested in dipole-dominated systems, we focus in the following on the case $\epsilon_{AA}^*=0.3$.

Corresponding mixture phase diagrams (finite $\Delta\mu^*$) are displayed in Fig. 9(a). It is seen that large, positive values of $\Delta\mu^*$ yield a topology characterized by one first-order isotropic-to-ferroelectric transition (see dashed lines), which is again very similar to what one finds for corresponding DHS-HS mixtures (cf. Fig. 6). A significant difference between Stockmayer and DHS-HS mixtures appears only at intermediate values of the chemical potential difference (e.g., $\Delta\mu^*=1.8$), where the additional *AA* attraction generates a *critical* point (CP) not present in the hard core systems. Its nature becomes clear when we consider the corresponding concentration-temperature diagram in Fig. 9(b), which shows that the two phases coexisting below the critical temperature differ mainly in c_A rather than in total density. Moreover, both of these phases are *unpolarized*, as seen more directly from Fig. 10 where the behavior of the polarization $P_{A,1}$

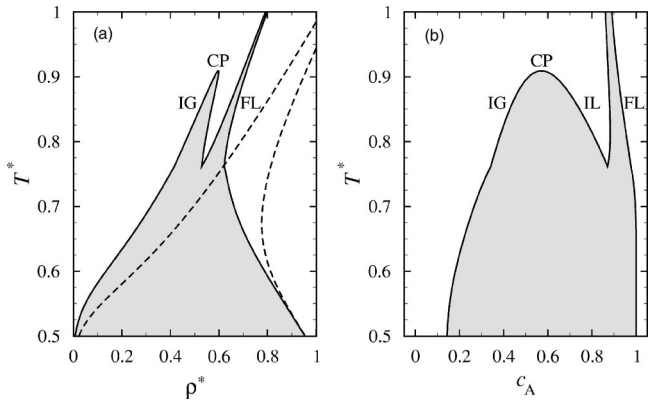

FIG. 9. MMF phase diagrams of Stockmayer/HS mixtures ($\Gamma=0$, $\epsilon_{AA}^*=0.3$). (a) Density-temperature diagrams at $\Delta\mu^*=1.8$ (solid lines) and $\Delta\mu^*=3.0$ (dashed lines). (b) Concentration-temperature diagram at $\Delta\mu^*=1.8$.

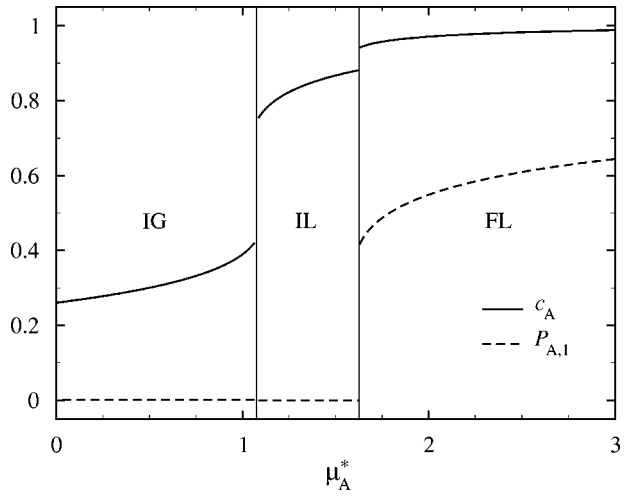

FIG. 10. Polarization and concentrations of *A* particles as functions of the chemical potential at $\Delta\mu^*=1.8$ and $T^*=0.85$ ($\Gamma=0$, $\epsilon_{AA}^*=0.3$).

$=(2/3)\alpha_{A,1}$ upon crossing the phase boundaries is plotted at a temperature in between the critical and the triple point IG-IL-FL. The two (lower-density) phases coexisting below the critical temperature are therefore a *B*-rich isotropic gas and an *A*-rich isotropic liquid, and we conclude that the critical point not displayed by the hard core systems is a demixing critical point within the isotropic phase.

The different phase behavior of Stockmayer/HS and DHS-HS mixtures within the MMF theory is also reflected by the different shapes of the phase boundary in the c_A-T^* diagram at *fixed* density $\rho^*=0.7$. Results for Stockmayer systems with $\Gamma=0$ and various finite interaction ratios (where the attraction parameters ϵ_{ab} have been chosen in proportion to the dipolar interactions) are plotted in Fig. 11 (see Fig. 7 for corresponding DHS results). Focusing on $\Gamma=0$ one observes a *maximum* in the phase boundary, which is in contrast to the monotonic c_A dependence of the transition temperatures for corresponding DHS-HS mixtures (cf. Fig. 7). The latter display only isotropic-to-ferroelectric transitions. Therefore, the maximum itself can be related to the occurrence of demixing without simultaneous polarization. From the same perspective, the absence of maxima at finite Γ in Fig. 11 suggests that these true Stockmayer mixtures transform directly into a polarized phase, as do the corresponding DHS mixtures within the MMF theory.

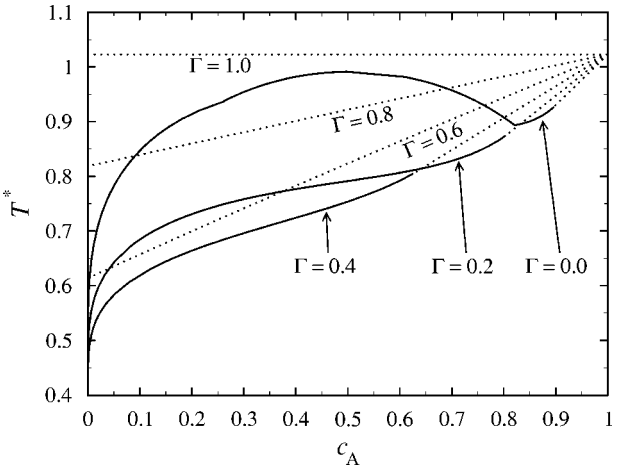

FIG. 11. MMF results for the temperatures related to the boundary of the isotropic phase for Stockmayer mixtures at $\rho^*=0.7$ and various values of Γ. The reduced LJ parameters ($\epsilon_{ab}^*:=\epsilon_{ab}\sigma^3/m_A^2$) are chosen as $\epsilon_{AA}^*=0.3$, $\epsilon_{BB}^*=0.3\,\Gamma$, and $\epsilon_{AB}^*=\epsilon_{BA}^*=0.3\sqrt{\Gamma}$. Dashed (solid) lines denote second-order (first-order) phase transitions.

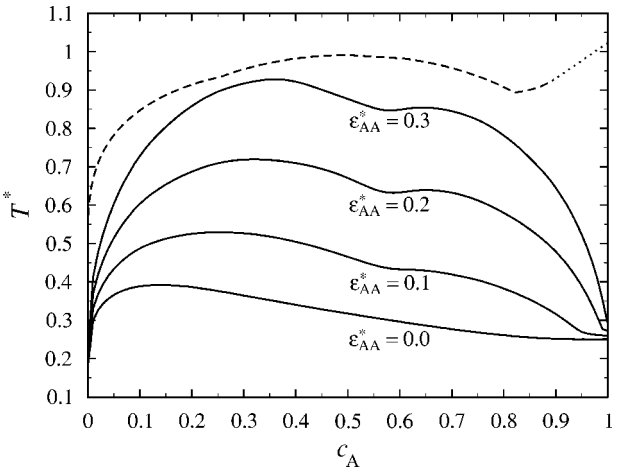

FIG. 12. RHNC results (solid lines) for the stability limits of Stockmayer/HS mixtures ($\Gamma=0$) at $\rho^*=0.7$ and various values of ϵ_{AA}^*. Also shown (dashed line) is the MMF result for the boundary of the isotropic phase at $\rho^*=0.7$ and $\epsilon_{AA}^*=0.3$.

Finally, turning back to the case $\Gamma=0$ (Stockmayer/HS mixture) it seems worthwhile to briefly compare our MMF results for the isotropic demixing transition to corresponding results from the RHNC theory. The latter predicts demixing to occur already in the absence of any dispersive interactions (cf. Sec. III A). The effect of adding such interactions (i.e., increasing ϵ_{AA}^* from zero) on the RHNC stability limits at $\rho^*=0.7$ is illustrated in Fig. 12. For all positive values of ϵ_{AA}^* investigated, concentration fluctuations are found to dominate in the whole range of compositions except in the immediate vicinity of $c_A=1,0$. Therefore, the maxima in the stability limits can indeed be related to true demixing transitions, and the shift of the curves indicates that attractive forces between *A* particles significantly raise the demixing temperatures. This is indeed plausible since increasing ϵ_{AA} implies that the interactions become more and more asymmetric and, consequently, demixing becomes more and more supported. A somewhat unexpected phenomenon is the appearance of a "notch" in the curves at $c_A\approx 0.55$, but this may be understood such that the tendency for demixing is somewhat less pronounced in mixtures with fairly symmetric composition (note that we are considering stability limits and *not* true coexistence curves where such notches would indicate the appearance of a triple point). Finally, focusing on the case $\epsilon_{AA}^*=0.3$ one sees that the RHNC results for the stability limit are, in fact, quite close to the boundary temperatures resulting from the MMF density-functional theory (see dashed line in Fig. 12). For these systems, results from the two approaches are therefore in fair agreement not only qualitatively, but also from a quantitative point of view.

IV. CONCLUSIONS

In this work we have employed RHNC integral equations and a mean-field-like density functional approach in order to investigate the appearance of demixing transitions in binary fluid mixtures of equisized dipolar spheres, where the two species differ only in the strength of the (point) dipole moment. Most of our results have been obtained for DHS systems characterized by the absence of any spherically symmetric attractive interactions. Thus, if any, it is the anisotropic dipolar interaction between the particles which can generate demixing transitions. Moreover, since pure DHS fluids tend to order ferroelectrically at sufficiently large densities and coupling strengths, a question of special importance was whether dense DHS *mixtures* can demix within the *isotropic* phase.

In order to solve that question within the RHNC approach we have applied a stability analysis based on the correlation functions (i.e., the fluctuations) in the isotropic fluid. Results have been obtained for DHS mixtures at a large (but still fluidlike) total density ($\rho^*=0.7$) which is in the range where the pure system spontaneously polarizes at sufficiently low temperatures. The same type of phase behavior is found to occur in moderately asymmetric DHS mixtures (i.e., large interaction parameters Γ), indicating that the tendency for ferroelectric ordering in these systems overwhelms any tendency to demix. The main difference to the pure system (at $\rho^*=0.7$) is then a monotonic *shift* of the isotropic-to-ferroelectric transition temperatures towards smaller values upon replacing strongly coupled *A* particles more and more by weakly coupled *B* particles. This is consistent with a recent low-temperature Monte Carlo study [32] where the degree of spontaneous polarization in DHS mixtures has been found to be much smaller than in the pure system. The RHNC fluctuations also indicate the ferroelectric transition to be accompanied by a change of composition such that the polarized phase is richer in the strongly coupled species.

Comparing these findings to MMF results at large Γ, which have been obtained previously by us in Ref. [23], it turns out that the much simpler MMF density-functional theory does indeed reproduce the phase behavior on a qualitative level, even though the actual ferroelectric transition temperatures are drastically overestimated (compared to the RHNC results, which are expected to be too high themselves). However, our present results show that even the qualitative consistency between the two approaches ends when one considers strongly asymmetric DHS mixtures characterized by small Γ. For these systems the RHNC analysis predicts demixing transitions to occur already *within* the isotropic phase (at intermediate concentrations c_A of the "stronger" component). This generalizes previously reported RHNC results [11,12] on (isotropic) demixing in DHS-HS mixtures ($\Gamma=0$), a phenomenon which has also been detected in recent computer simulations [10]. Within the MMF approach, on the other hand, the isotropic demixing transition is absent, and the mixtures display only isotropic-to-ferroelectric transitions even at $\Gamma=0$. Given the severe approximations within the MMF we conclude that demixing transitions in dipolar mixtures without any dispersive interactions, as observed in the RHNC, are in fact highly nontrivial effects driven essentially by interparticle *correlations* rather than by the anisotropic dipolar interaction itself.

Finally, we have shown that RHNC and MMF results do become consistent again for mixtures where the dipolar interactions are supplemented by dispersive—i.e., *spherically symmetric* and *attractive* interactions. Specifically, considering a mixture of Stockmayer spheres (*A*) and hard spheres (*B*) we have found that the MMF recovers demixing within the isotropic phase (as does the RHNC) even if the isotropic attraction between *A* particles is so small that the pure *A* fluid does not display conventional vapor-liquid coexistence. This sensitivity may indicate that dispersive interactions play a similar important role for demixing transitions in dipolar mixtures, as they do in the context of vapor-liquid coexistence of pure dipolar fluids.

ACKNOWLEDGMENTS

S.H.L.K. acknowledges financial support from the Deutsche Forschungsgemeinschaft through the Emmy-Noether Program.

APPENDIX: DIELECTRIC CONSTANT OF THE DIPOLAR MIXTURE

In this appendix we give a brief derivation of expression (2.11) for the dielectric constant of the dipolar mixture. We start from the two-component generalization of Kirkwood's formula [33]—that is,

$$\frac{(\epsilon-1)(2\epsilon+1)}{\epsilon}=4\pi\beta\sum_{ab}\sqrt{\rho_a\rho_b}m_a m_b\, g^{\mathrm{K}}_{ab}, \tag{A1}$$

where the g^{K} factors are given by

$$g^{\mathrm{K}}_{ab}=\delta_{ab}-\frac{1}{3}\sqrt{\frac{\rho_a\rho_b}{12\pi}}\,\tilde{h}^{ab}_{110}(0). \tag{A2}$$

In Eq. (A2), $\tilde{h}^{110}_{ab}(0)=4\pi\int dr r^2\, h^{110}_{ab}(r)$ and $h^{110}_{ab}(r)$ is the (dipole-dipole) projection of the total correlation function between a and b in a space-fixed coordinate system. Using standard relations (see Appendix 3B in Ref. [24]) between the space-fixed frame and the **k** frame employed in the present work one finds

$$g^{\mathrm{K}}_{ab}=\frac{1}{3}\sum_{\chi=-1}^{1}\left(\delta_{ab}+(-1)^{\chi}\frac{\sqrt{\rho_a\rho_b}}{3}\tilde{h}^{11,\chi}_{ab}(0)\right). \tag{A3}$$

We now make use of the exact Ornstein-Zernike relations [12] for the mixture. For the coefficients of interest these imply

$$\delta_{ab}+(-1)^{\chi}\frac{\sqrt{\rho_a\rho_b}}{3}\tilde{h}^{11,\chi}_{ab}(0)=[(\mathbf{F}_{\chi})^{-1}]_{ab}, \tag{A4}$$

where the right-hand side involves elements of the inverse of the matrices defined in Eqs. (2.10). Equations (A4) allow us to express the g^{K} factors in terms of the direct correlation functions—that is

$$g_{ab}^{\mathrm{K}} = \frac{1}{3}\{[(\mathbf{F}_0)^{-1}]_{ab} + 2\,[(\mathbf{F}_1)^{-1}]_{ab}\}. \tag{A5}$$

The next transformation involves the prefactors of the g_{ab}^{K} appearing in Eq. (A1). Generalizing corresponding relations for one-component dipolar fluids [see Eq. (C8) in Ref. [16]] one obtains

$$\frac{4\pi}{3}\beta\sqrt{\rho_a\rho_b}m_a m_b = -\sqrt{\rho_a\rho_b}\sqrt{\frac{5}{4\pi}}\,\tilde{c}_{ab}^{112}(0) = [\mathbf{F}_0]_{ab} - [\mathbf{F}_1]_{ab}. \tag{A6}$$

Combining Eqs. (A1), (A5), and (A6) yields the relation

$$\frac{(\epsilon-1)(2\epsilon+1)}{\epsilon} = 2\,\mathrm{Tr}\mathbf{Z} - \mathrm{Tr}(\mathbf{Z}^{-1}) - 2, \tag{A7}$$

where we have introduced the product matrix $\mathbf{Z}=\mathbf{F}_0(\mathbf{F}_1)^{-1}$, and "Tr" denotes the trace. In order to proceed towards the simpler relation (2.11) for ϵ we first show that one of the two eigenvalues of $\mathbf{Z}$ is *identically one*. The central equation is again Eq. (A6) since it implies the relation

$$\det(\mathbf{F}_0 - \mathbf{F}_1) = 0 \tag{A8}$$

and, consequently,

$$\det(\mathbf{Z} - 1) = \det[(\mathbf{F}_0 - \mathbf{F}_1)(\mathbf{F}_1)^{-1}] = \frac{\det(\mathbf{F}_0 - \mathbf{F}_1)}{\det\mathbf{F}_1} = 0. \tag{A9}$$

It follows now immediately that one of the eigenvalues of $\mathbf{Z}$ is identically 1. This property in turn implies

$$\mathrm{Tr}\mathbf{Z} = \det\mathbf{Z} + 1,$$

$$\mathrm{Tr}\mathbf{Z}^{-1} = (\det\mathbf{Z})^{-1} + 1, \tag{A10}$$

where we have used the fact that the trace and determinant are equivalent to the sum and product of the eigenvalues, respectively (plus the fact that $\mathbf{Z}$ is a 2×2 matrix). Inserting Eqs. (A10) into Eq. (A7) and identifying corresponding terms on the left- and right-hand sides of the resulting equation one finally obtains

$$\epsilon = \det\mathbf{Z}, \tag{A11}$$

which leads immediately to Eq. (2.11).

[1] J.-J. Weis, D. Levesque, and G. J. Zarragoicoechea, Phys. Rev. Lett. **69**, 913 (1992).
[2] J.-J. Weis and D. Levesque, Phys. Rev. E **48**, 3728 (1993).
[3] D. Wei and G. N. Patey, Phys. Rev. Lett. **68**, 2043 (1992).
[4] D. Wei and G. N. Patey, Phys. Rev. A **46**, 7783 (1992).
[5] M. E. van Leeuwen and B. Smit, Phys. Rev. Lett. **71**, 3991 (1993).
[6] J.-J. Weis and D. Levesque, Phys. Rev. Lett. **71**, 2729 (1993).
[7] D. Levesque and J.-J. Weis, Phys. Rev. E **49**, 5131 (1994).
[8] J. M. Tavares, J.-J. Weis, and M. M. Telo da Gama, Phys. Rev. E **59**, 4388 (1999).
[9] T. Tlusty and S. A. Safran, Science **290**, 1328 (2000).
[10] M. J. Blair and G. N. Patey, Phys. Rev. E **57**, 5682 (1998).
[11] X. S. Chen, M. Kasch, and F. Forstmann, Phys. Rev. Lett. **67**, 2674 (1991).
[12] X. S. Chen and F. Forstmann, Mol. Phys. **76**, 1203 (1992).
[13] *Ferrofluids, Magnetically Controllable Fluids and their Applications*, edited by S. Odenbach, Lecture Notes in Physics Vol. 594 (Springer-Verlag, Berlin, 2002).
[14] G. T. Gao, J. B. Wollert, X. C. Zeng, and W. Wenchuan, J. Phys.: Condens. Matter **9**, 3349 (1997).
[15] R. J. Sadus, Mol. Phys. **87**, 979 (1996).
[16] S. Klapp and F. Forstmann, J. Chem. Phys. **106**, 9742 (1997).
[17] D. Wei, G. N. Patey, and A. Perera, Phys. Rev. E **47**, 506 (1993).
[18] M. Kinoshita and M. Harada, Mol. Phys. **79**, 145 (1993).
[19] X. S. Chen, F. Forstmann, and M. Kasch, J. Chem. Phys. **95**, 2832 (1991).
[20] B. Groh and S. Dietrich, Phys. Rev. E **50**, 3814 (1994).
[21] B. Groh and S. Dietrich, Phys. Rev. Lett. **72**, 2422 (1994).
[22] E. Lomba, J.-J. Weis, N. G. Almarza, F. Bresme, and G. Stell, Phys. Rev. E **49**, 5169 (1994).
[23] G. M. Range and S. H. L. Klapp, Phys. Rev. E **69**, 041201 (2004).
[24] C. G. Gray and K. E. Gubbins, *Theory of Molecular Fluids*, The International Series of Monographs on Chemistry Vol. 1 (Clarendon, Oxford, 1984).
[25] J. G. Kirkwood and F. P. Buff, J. Chem. Phys. **19**, 774 (1951).
[26] J. P. Hansen and I. R. McDonald, *Theory of Simple Liquids* (Academic, London, 1976).
[27] L. Verlet and J.-J. Weis, Phys. Rev. A **5**, 939 (1972).
[28] P. H. Fries and G. N. Patey, J. Chem. Phys. **82**, 429 (1985).
[29] N. F. Carnahan and K. E. Starling, J. Chem. Phys. **51**, 635 (1969).
[30] P. Frodl and S. Dietrich, Phys. Rev. A **45**, 7330 (1992).
[31] M. E. van Leeuwen, Fluid Phase Equilib. **99**, 1 (1994).
[32] B. J. Costa Cabral, J. Chem. Phys. **112**, 4351 (2000).
[33] J. S. Høye and G. Stell, J. Chem. Phys. **70**, 2894 (1979).